Chapter 4

Large-Scale Sensor Network using Fiber laser Scheme

4.1 Intensity and Wavelength Division Multiplexing Sensor System

A simple method for interrogating WDM-FBG sensors is by using a tunable laser source to dynamically sweep the whole FBGs' wavelength range. In contrast with the broadband source, a laser source provides a higher power within a narrow spectral width and thus improves the signal to noise ratio (SNR) [1]. These merits allow us for a larger number of FBG sensors with the same Bragg wavelengths if we take advantage of a tunable laser incorporated with the IWDM technique. In this section, we propose an IWDM-FBG sensor system using a tunable multiport EDF ring laser. The output terminals of the fiber laser are constructed by using a 2x4 coupler that comprises three fiber couplers with different coupling ratios. All the sensing FBGs connected at the three different terminals can have the approximately equal peak reflectivities and it is unnecessary for us to fabricate specified peak reflectivities of FBGs for intensity multiplexing. Consequently, the proposed multiport fiber laser can easily increase the capacity of a FBG sensor system by using the IWDM technique.

4.1.1 Principles

Figure 4.1 schematically shows the IWDM-FBG sensor system. The light source of this sensor system is a tunable fiber ring laser with a Fabry-Perot filter for wavelength selection. For the IWDM technique, the laser output consists of three ports of a 2x4 coupler that is connected by three fiber couplers with different coupling ratios. The output ratio between the different lasing branches can be designed according to the coupling ratios of the three fiber couplers. The lasing light from each output port is launched into a branch of sensing FBG chain. In WDM technique, the multiplexing number of the sensing gratings is limited by the reflective band of each FBG sensor and the whole bandwidth of the light source. Therefore, the wavelengths of sensing gratings cannot cross each other. On the contrary, our proposed scheme for the IWDM technique allows the peak reflectivity of each grating at different lasing branches crossing each other. When spectral overlap occurs between two sensing gratings, the output intensity is the sum of each grating's output intensity. As a result, the overlap output still can be used to address the sensing information without the un-measurable gap.

4.1.2 Experimental results and Discussion

The fiber laser was constructed by a 2x4 coupler, a Fabry-Perot filter with 44-nm tunable range, and a commercial EDFA. The 2x4 fiber coupler comprised a 2×2 fiber coupler with coupling ratio 50:50, 1×2 coupler with coupling ratio 40:60, and 1×2 coupler with coupling ratio 20:80. The lasing light traveled through the 2×4 fiber coupler and split into three FBG branches

(FBG1=1545.32nm, FBG2=1548.32nm, FBG3=1550.28nm) for experimental demonstration of our proposed multiplexing technique. Because of the 2×4 coupler, the power ratio launched into FBG1, FBG2, and FBG3 was 30%: 20%: 10%. The peak reflectivity of each FBG was 99%. The backreflected light from each FBG finally propagated through the 2×4 coupler and into the photo detector (PD). The output signal from each PD was fed into a microprocessor to accurately calculate the backreflected wavelength.

Fig. 4.2 shows the output from the 30% lasing port when we turned the Fabry-Perot filter by using a voltage controller from 0V to 12V. This operating voltage range can select the lasing wavelength within the working range from 1528nm to 1572nm. The average power from this 30% output port is 9.16dBm. Fig. 4.3 shows the laser stability from this 30% lasing port within fifteen minutes. When the central wavelength of the laser is 1533.19 nm, the average wavelength variation is 0.04 nm. In addition, the variation of the output power is $(P_{\max} - P_{\min})/\overline{P}_{out} = 0.64\%$, where $P_{\max}$ is the maximum output power, $P_{\min}$ is the minimum output power, and $\overline{P}_{out}$ is the average output power. The system stability of this IWDM system is determined by these two parameters and the adopted method for electronic signal processing, which will be discussed in the next section.

Fig. 4.4 shows the output power of the 30%, 20% and 10% output ports at different lasing wavelengths. The average output power from the 20% and 10% lasing port are 7.30 dBm and 4.26 dBm, respectively. The maximum power variation is 0.55dB from 1528nm to 1572nm. Fig. 4.5 shows the output spectra of the 30%, 20% and 10% output ports at different lasing wavelengths. For quasi-static strain sensing, we drove the Fabry-Perot filter by using a scanning

sawtooth waveform to sweep the wavelength range of the sensing FBGs. Fig. 4.6 shows the output signal from the PD under the scanning Fabry-Perot operation. Finally, in contrast with a broadband source, the light source of our proposed sensor system is a tunable fiber laser, which can enhance the SNR and the sensing resolution for the system. These advantages facilitate the accurate measurement that is sufficiently reliable against the noisy environments, especially for the long-distance remote sensing in a smart structure.

In this section, we focus our attention on the IWDM laser source for a high-capacity and long-distance sensor system. Nevertheless, how to distinguish the reflected signal encoded via IWDM has been reported previously [2]. In the previous study, the technique of a minimum variance shift (MVS) has been proposed for the discrimination of IWDM signals. The MVS technique is based on the construction of a variable spectrum from the original uncontaminated spectra of the FBGs. According to the MVS technique, if there is wavelength overlap due to two or three FBG sensors from different ports, the reflected power will be accumulated. Such accumulated intensity information must also be encoded. Moreover, our proposed fiber laser with lasing range from 1528 nm to 1572 nm is capable of supporting 22 WDM channels with 2 nm per channel. The measurement range for each sensing FBG on the identical sensing branch therefore has to be smaller than [0, 1760] $\mu\varepsilon$. Because there are three intensity-coded branch, the allowable number of FBGs is $22 \times 3 = 66$. The IWDM system can support only few intensity-coded branches because the MVS technique is time-consuming. In addition, the scanning rate of the tunable filter always limits the dynamic range of the sensor system if the FBGs undergo

the noise perturbation from the environments. For this problem we should use the MVS technique in conjunction with a time-interval counting method, which is usually used for the perturbation problem in a conventional WDM scheme [3-5]. Nevertheless, the IWDM scheme can easily double or triple the sensing number based on the WDM technology and maintain the measurable range for each sensor.

Another problem when wavelength overlap occurs is the coherence related problems which could be overcome by using the following methods: (a) We can add long fibers between the three-port coupler and the FBGs such that our proposed system could be used for long-distance sensing. (b) We can use a phase modulator to degrade the coherence of the lasing light.

In summary, an IWDM-FBG sensor system using a tunable multiport fiber ring laser is proposed and experimentally demonstrated in this section. Such a multiplexing technique can easily increase the capacity of a FBG sensor system. In the experiment, a three-point sensor system was shown. The experimental results show that our proposed fiber ring laser can simultaneously lase three outputs with different intensity for the information addressed by the IWDM technique. Moreover, the laser source can enhance the SNR and resolution of the IWDM sensor system.

4.2 Linear-Cavity Fiber Raman Laser

In this section, we propose a FBG sensor on the basis of a liner-cavity fiber Raman laser. The linear cavity is constructed by two FBGs combined with a

fiber loop mirror; and a section of 25-km non-zero dispersion shifted fiber is used for the Raman gain. In our experiment, such a dual-wavelength fiber Raman laser sensor provided a high optical SNR up to 50 dB even if two FBGs were located at 25-km remote sensing points. In addition, each peak power was stable even if a strain was imposed on one of the FBGs. These features can facilitate a long-haul or a large-scale fiber sensor system and can be easily extended for multipoint sensing applications. Furthermore, we can directly construct a dynamic FBG sensor system by using our proposed FBG Raman sensor incorporated with a fixed filter as a fast wavelength interrogator [6]. The dynamic range of such a large-scale sensor system therefore would not be restricted by a tunable filter.

4.2.1 Experiment setup

The schematic diagram of the proposed long-distance FBG sensor system is shown in Fig. 4.7. The fiber Raman laser comprises a fiber loop mirror acting as one of the cavity mirror with a fixed reflectivity, a section of 25-km non-zero dispersion shifted fiber (NZDSF) pumped by the 1450-nm Raman pump, and a series of FBGs simultaneously acting as another cavity mirrors and sensing elements. The lasing multiwavelength is determined by the sensing FBG chain and the lasing output leaks from the fiber loop mirror. Here the fiber loop mirror is constructed by a piece of 2-m single mode fiber, a polarization controller (PC), and a 2×2 optical coupler (C). Both the polarized direction of PC and the coupling ratio of coupler can be used to adjust a suitable reflectivity for the loop mirror. Furthermore, the Raman pump for this fiber laser consists of two 1450 nm laser diodes (LD). The outputs from the two lasers at the pump wavelength are combined by using a polarization beam combiner (PBC) to

result in a depolarized output. The output combined from two laser diodes is launched into the laser cavity via the WDM coupler multiplexing 1550-nm band signals and 1450 nm band pumps. This pump light is then absorbed by the 25-km NZDSF, which has mode field area A_{eff} =73.7 m^2, 1497-nm zero dispersion wavelength, and 5-dB loss at 1550-nm wavelength. Fig. 4.8 (a) shows the experimental setup for the Raman gain measurement. The tunable laser (TL) with a tunable wavelength range of 1530-1570 nm at a power of –10 dBm was fed into the 25 km NZDSF. The Raman pump launched into NZDSF was 330 mW at 1450 nm. Fig. 4.8 (b) shows the Raman gain at different signal wavelength. The maximum Raman gain is 8.45 dB at 1548 nm. The Raman gain spectrum depends on the index profile of the fiber [7]. Furthermore, the Raman amplifier is the inhomogeneous broadened gain. Therefore, the Raman gain spectrum is similar even if we increase the number of input signal wavelength. The saturation power of the Raman amplifier is much larger compared with that of other optical amplifiers. In Ref. [8], the Raman pump launched into 10 km dispersion shifted fiber was 2.8 W at 1455 nm. The Raman gain decreased when the input signal power increased. Finally, the saturated output power was 1.4 W [8].

4.2.2 Experimental results and Discussion

In our experiment, we examined two sensing FBGs and achieved a dual-wavelength fiber Raman laser for the proposed long-distant sensor system. The Bragg wavelengths of FBG1 and FBG2 were 1544.69 and 1558.91 nm. Both the peak reflectivities of the FBGs were approximately 99% and their average 3dB bandwidth were 0.45 nm. The Raman pump with 330-mW output

power pumped the NZDSF via a 1450/1550 nm WDM coupler. The coupling ratio of the 2×2 coupler (C) for the laser output was 30:70 leading to its reflectivity 84 %. Under these conditions, the linear-cavity Raman laser lased a continuous wave with dual-wavelength at 1544.69 and 1558.91 nm simultaneously. Fig. 4.9 (a) shows the output spectrum of this linear-cavity Raman laser. The optical SNRs provided by FBG1 and FBG2 for the sensor system were over 50 dB even if the two sensing points were located 25-km far from the OSA. Fig. 4.9 (b) shows the wavelength shifts of FBG2 when a strain was imposed on it. There was no influence on the lasing wavelength of FBG1 when the wavelength of FBG2 drifted. Fig. 4.10 shows the strain measurement of the FBG2. The FBG2 was strained in steps of 80 με up to 2000 με, which is equivalent to 2.27 nm of the wavelength shift. Resolution of the sensor system was determined by the OSA resolution of 0.01 nm. The peak power variation of the Raman laser as a function of time is shown in Fig. 4.11. The fluctuations of the dual-wavelength peaks were both smaller than 0.35 dB. Such a lasing output is stable and intense enough for the long-distant fiber sensor system. Moreover, to present the lasing mechanism for the dual-wavelength operation, in Fig. 4.12 we illustrate the peak power of the Raman laser as a function of the pump power. The pumping threshold of FBG1 and FBG2 were 270 mW and 280 mW approximately. After the pump power was larger than this threshold, the two wavelength outputs lased stably and were suitable for our proposed sensor system. The wavelength action range for this Raman laser depends on the cavity loss and the Raman gain at different wavelength. In the previous study [9], when the Raman pump launched into 9 km dispersion shifted fiber was 1.1 W, the Raman laser action range was up to 18 nm.

In this section, we concentrate our study on the FBG sensor system using a linear-cavity fiber Raman laser scheme. Thus we only used an OSA to measure the lasing wavelength. The dynamic strain measurement could be improved by using a better wavelength interrogator [6]. In addition, the main limitation on the maximum distance and number for the sensors would be the gain medium. The Raman gain can be improved by using the dispersion compensating fiber to increase the Raman gain efficiency [7, 10] and by increasing the Raman pump power. Moreover, we can use multiwavelength Raman pump to increase the gain bandwidth. The 100nm flat gain bandwidth has been reported [10].

In summary, a long-distance FBG sensor system using a linear-cavity fiber Raman laser scheme was proposed. Because of the inhomogeneous broadening of the Raman gain, the proposed fiber laser can generate multiwavelength lasing output for multipoint sensing at a long distance. Experimental results showed a dual-wavelength fiber Raman laser with stable and intense peak power even if the FBGs were located at a 25-km far sensing position. The proposed fiber laser sensor system can be used for large-scale or long-haul smart structures.

4.3 Fiber Ring Laser with EDWA and SOA

Erbium-doped waveguide amplifiers (EDWAs) are now very attractive for used in metro networks due to their compactness, low processing cost, and compatibility with other optical devices. Furthermore, the EDWAs have the advantage of the fundamental qualities of the EDFAs, such as a low noise figure, negligible polarization dependence, and the absence of inter-channel

crosstalk. Moreover, they have potential to be integrated with pump lasers and other optical devices [11-13]. In this section, a FBG sensor system in the fiber ring laser scheme with a hybrid amplifier as gain medium is proposed. The ring cavity comprises a series of FBGs and a 25-km single mode fiber (SMF); both EDWA and SOA are employed as the gain medium. In this experiment, this multiwavelength fiber laser scheme provided a high optical SNR over 50 dB, even when FBGs were located at 25 km remote sensing points. Additionally, the peak power of each lasing wavelength was stable, even when different strains were imposed on the FBG. These features can facilitate a long-distance or large-scale fiber sensor system and can be easily extended for multipoint sensing applications.

4.3.1 Experiment Setup

Figure 4.13 shows the schematic diagram of the proposed long-distance FBG sensor system. The fiber ring laser comprises a hybrid amplifier with an EDWA and an SOA, a circulator (OC), a 1x2 optical coupler with a coupling ratio of 90:10 (C), a 25 km section of SMF, and a series of FBGs simultaneously acting as cavity mirrors and sensors. The lasing wavelength is derived by the sensing FBG chain. The EDWA is manufactured by Teem Photonics via a two-step ion-exchange process. It has a saturated output power of about 10 dBm and an amplified spontaneous emission (ASE) power of 3 mW. The SOA has a saturated output power of about 13.7 dBm and an ASE power of 3.4 mW. In the fiber-laser-based sensor system, the principal limitation on the maximum distance separating the sensors and number of sensors is the gain medium. To evaluate the performance of this proposed hybrid amplifier, a tunable laser and an optical spectrum analyzer (OSA) are used to measure its gain spectra. Figure

4.14 shows the gain spectra of the amplifiers. Input power was set at -25 dBm. The maximum gain of the hybrid amplifier was 36.71 dB at 1532 nm. In contrast to the single EDWA or SOA, the hybrid amplifier had a higher gain. Furthermore, this hybrid amplifier can facilitate a long-distance or large-scale fiber sensor system. Moreover, for a long-distance sensor system, the light source with high output power is required. The ASE power of amplifiers was measured. Figure 4.15 shows the ASE spectra of EDWA and hybrid amplifier. The ASE power from EDWA was only 3 mW. However, the hybrid amplifier increased ASE power from 3 mW to 23.2 mW.

4.3.2 Experimental Results and Discussion

In this experiment, three sensing FBGs were examined. These three sensing FBGs generated a triple-wavelength fiber laser for the proposed long-distance sensor system. The Bragg wavelengths of FBG1, FBG2, and FBG3 were 1552.52, 1554.47, and 1556.53 nm, respectively. The peak reflectivity for each FBG sensor was approximately 99%. Under these conditions, the fiber ring laser with the proposed hybrid amplifier lased a continuous wave with three wavelengths simultaneously. Fig. 4.16 (a) shows the output spectrum of this fiber laser. The optical SNRs provided by FBG1, FBG2, and FBG3 for the sensor system were over 50 dB, even when the three sensing locations were 25 km from the optical spectrum analyzer. The peak power of lased output at triple-wavelength was approximately -13.3 dBm. To compare the characteristics of different gain media, an experiment with only the SOA incorporated into the laser cavity was performed. Fig. 4.16 (b) shows the output spectrum of this fiber laser with only the SOA. The optical SNRs and peak

power were only around 22 dB and -47.1 dBm, respectively, because the SOA did not have sufficient gain and power to generate multiwavelength oscillations.

Figure 4.17 shows the wavelength shifts of FBG3 when different strains were imposed on it. There was no influence on the lasing wavelengths for FBG1 and FBG2 when the wavelength of FBG3 drifted. Fig. 4.18 shows the peak power variations of the fiber laser as a function of time. The fluctuations of the lasing peaks were less than 0.58 dB. Such a lasing output is stable and sufficiently intense for the long-distant fiber sensor system.

In summary, this investigation proposed a long-distance FBG sensor system using a fiber ring laser with an EDWA and an SOA. Owing to the inhomogeneous broadening of the hybrid amplifier and the high ASE power, the proposed fiber laser generated multiwavelength output for multipoint sensing at a long distance. Experimental results demonstrated that the multiwavelength fiber laser generated stable and intense peak power, even when the FBGs were at a location of 25 km. Furthermore, employing EDWA made the system more compact and has potential for integrating the system into planar waveguides. The proposed fiber sensor system can be used for long-distance or large-scale smart structures.

References

[1] C. C. Chan, W. Jin, H. L. Ho, and M. S. Demokan, “Performance analysis of a time-division-multiplexed fiber Bragg grating sensor array by use of a tunable laser source” *IEEE Journal of Selected Topics in Quantum Electronics*, vol. 6, pp. 741-749, 2000.

[2] C. C. Chan, C. Z. Shi, J. M. Gong, W. Jin, and M. S. Demokan, "Enhancement of the measurement range of FBG sensors in a WDM network using a minimum variance shift technique coupled with amplitude-wavelength dual coding," *Optics Communications*, vol. 215, pp. 289-294, 2003.

[3] S. H. Yun. D. J. Richardson, and B. Y. Kim, "Interrogation of fiber grating sensor arrays with a wavelength-swept fiber laser," *Optics Letters*, vol. 23, pp. 843-845, 1998.

[4] Y. Yu, L. Lui, H. Tam, and W. Chung, "Fiber-laser-based wavelength-division multiplexed fiber Bragg grating sensor system", *IEEE Photonics Technology Letters*, vol. 13, pp. 702-704, 2001.

[5] J. M. Gong, J. M. K. MacAlpine, C. C. Chan, W. Jin, M. Zhang, and Y. B. Liao, "A Novel wavelength detection technique for fiber Bragg grating sensors," *IEEE Photonics Technology Letters*, vol. 14, pp. 678-680, 2002.

[6] Y. Sano and T. Yoshino, "Fast optical wavelength interrogator employing arrayed waveguide grating for distributed fiber Bragg grating sensors," *Journal of Lightwave Technology*, vol. 21, pp.132-139, 2003.

[7] J. Bromage, K. Rottwitt, and M. E. Lines, "A Method to predict the Raman gain spectra of germanosilicate fibers with arbitrary index profiles," *IEEE Photonics Technology Letters*, vol. 14, pp. 24- 26, 2002.

[8] S. A. E. Lewis, S. V. Chernikov, and J. R. Taylor, "1.4 W saturated output power from a fibre Raman amplifier," *Optical fiber communication conference* (OFC'99), vol. 2, pp. 114 -116, 1999.

[9] F. Koch, P. C. Reeves-Hall, S. V. Chernikov, and J. R. Taylor, "CW, multiple wavelength, room temperature, Raman fiber ring laser with external 19 channel, 10 GHz pulse generation in a single electro-absorption

modulator," *Optical fiber communication conference* (OFC2001), vol. 3, pp. WDD7-1-WDD7-3, 2001.

[10] S. Namiki and Y. Emori, "Ultrabroad-band Raman amplifiers pumped and gain-equalized by wavelength-division-multiplexed high-power laser diodes," *IEEE Journal of Selected Topics in Quantum Electronics*, vol. 7, pp. 3-16, 2001.

[11] K. C. Reichmann, P. P. Ianonne, M. Birk, N. J. Frigo, D. Barbier, C. Cassagnettes, T. Garret, A. Verlucco, S. Perrier, J. Philipsen, "An Eight-Wavelength 160-Km Transparent Metro WDM Ring Network Featuring Cascaded Erbium-Doped Waveguide Amplifiers," *IEEE Photonics Technology Letters*, vol. 13, pp. 1130 - 1132, 2001.

[12] Y. Jaouën, L. D. Mouza, D. Barbier, J.-M. Delavaux, and P. Bruno, "Eight-Wavelength Er-Yb Doped Amplifier: Combiner / Splitter Planar Integrated Module," *IEEE Photonics Technology Letters*, vol. 11, pp. 1105 - 1107, 1999.

[13] P. G. Kik and A. Polman, "Erbium-doped optical waveguide amplifiers on silicon," *MRS Bulletin*, pp. 48-54, Apr. 1998.

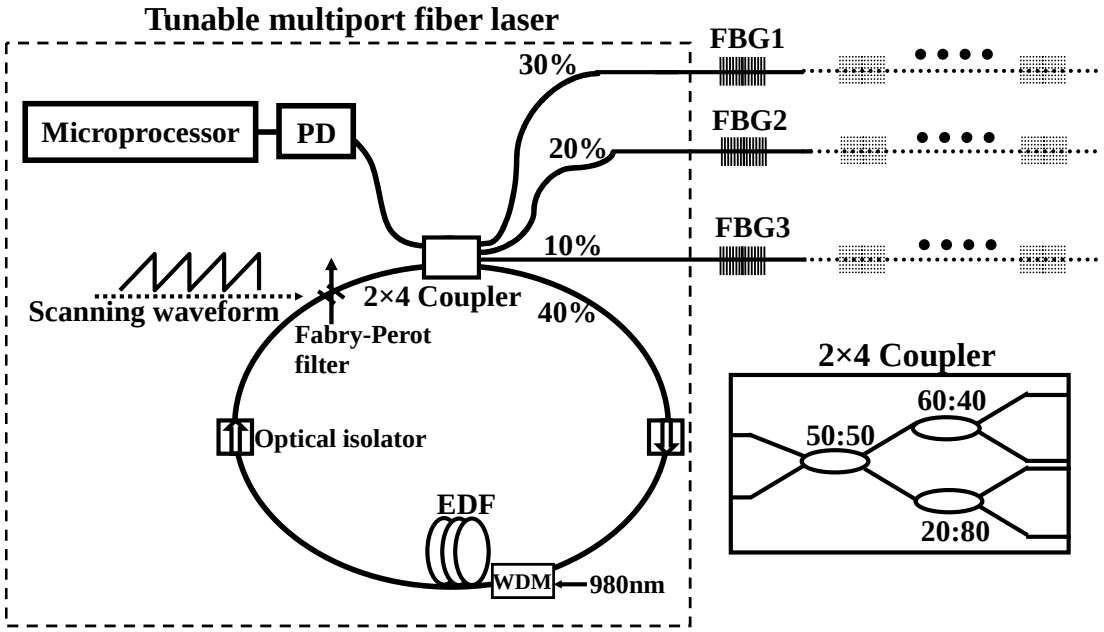

Fig. 4.1 Schematic diagram of the tunable multiport fiber laser for IWDM sensor systems. (PD: Photo detector, EDF: Erbium doped fiber, WDM: 980/1550 WDM coupler)

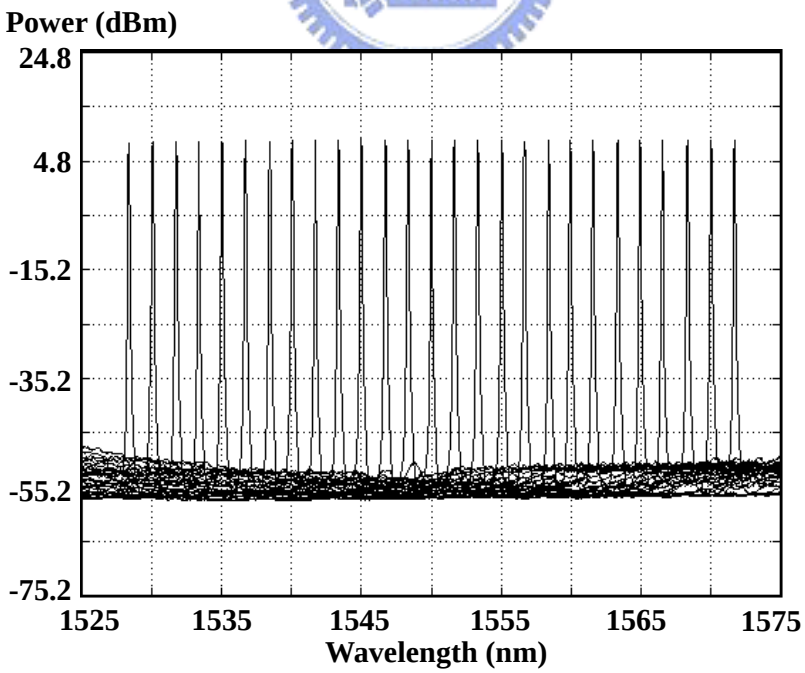

Fig. 4.2 Output spectra at 30% lasing port within the working range from 1528nm to 1572nm.

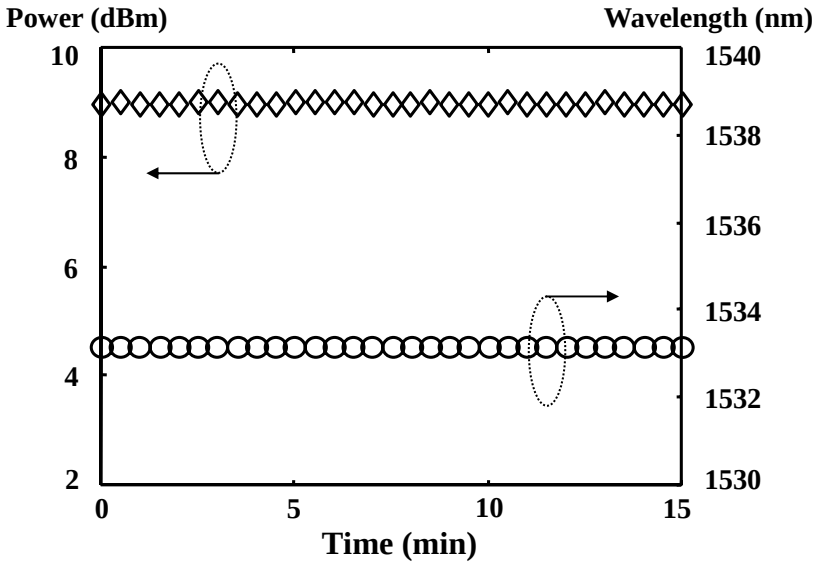

Fig. 4.3 Laser stability regarding output power variation and wavelength drift at 1533.19 nm.

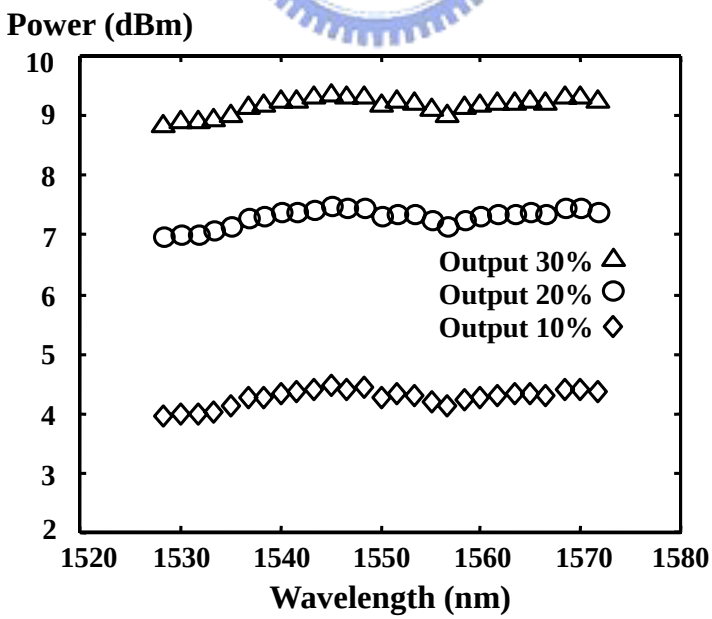

Fig. 4.4 Output powers of the 30%, 20% and 10% lasing ports at different lasing wavelengths.

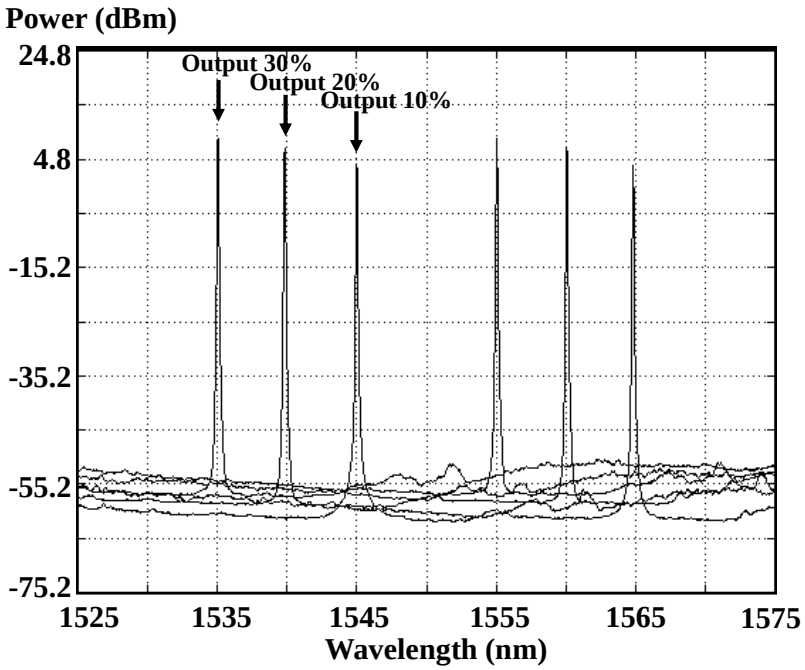

Fig. 4.5 Output spectra of the 30%, 20% and 10% lasing ports at different lasing wavelengths.

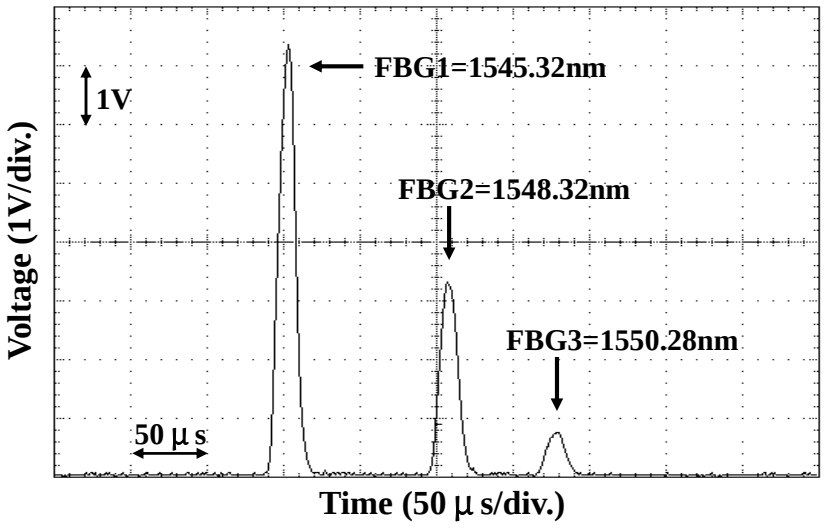

Fig. 4.6 Output signals from the PD under the scanning Fabry-Perot filter operation. (Vertical scale is 1V/div. Horizontal scale is 50 μ s/div.)

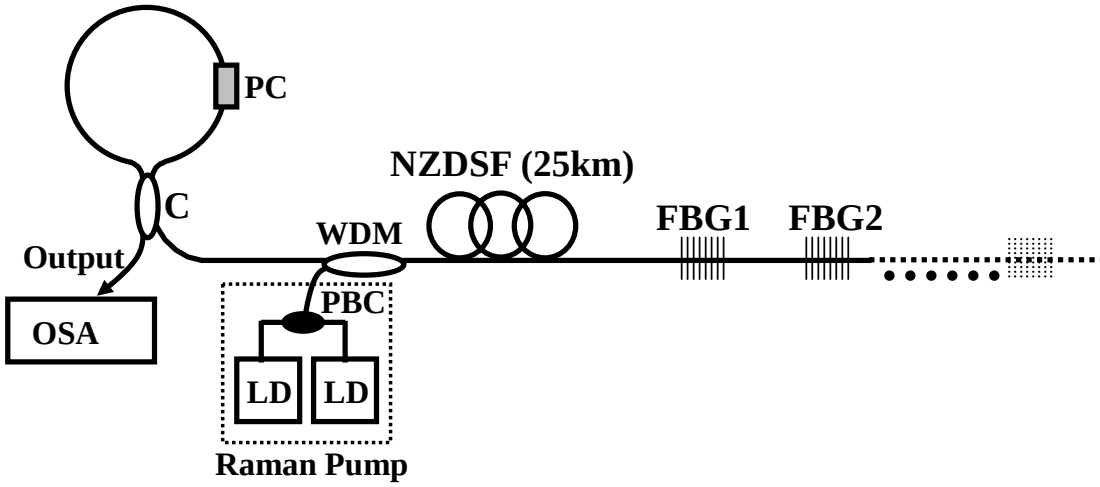

Fig. 4.7 Schematic diagram of the long-distance FBG sensor system. (PC: Polarization controller, C: 2x2 coupler, NZDSF: non-zero dispersion shifted fiber, PBC: polarization beam combiner, LD: 1450nm laser diode, WDM: 1450/1550nm WDM coupler, FBGs: fiber Bragg gratings, OSA: optical spectrum analyzer).

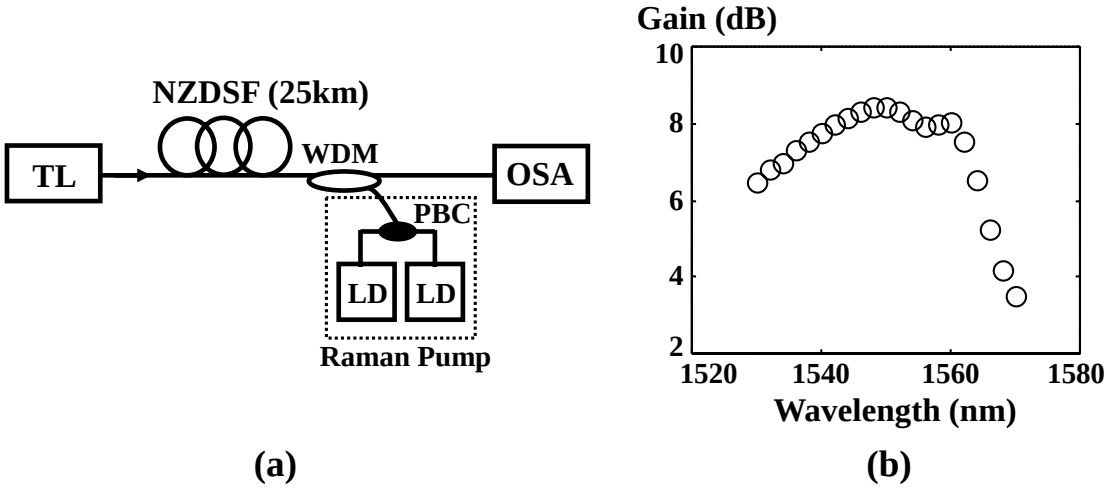

Fig. 4.8 (a) Schematic diagram of the Raman gain measurement. (b) Raman gain at different signal wavelength. (TL: tunable laser)

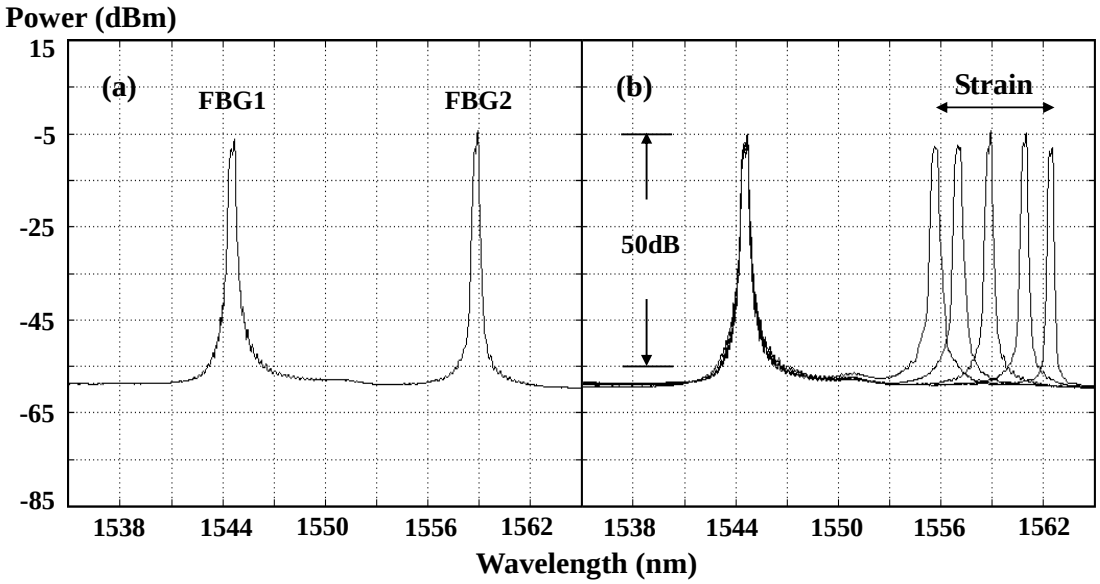

Fig. 4.9 Output spectra of the linear-cavity fiber laser with 330-mW pump power (a) when no strain was applied (b) when strain was applied to FBG2.

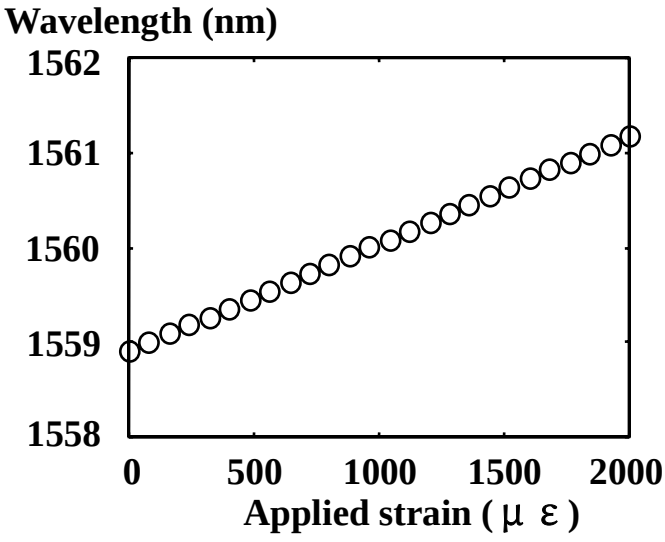

Fig. 4.10 The strain measurement of the FBG2.

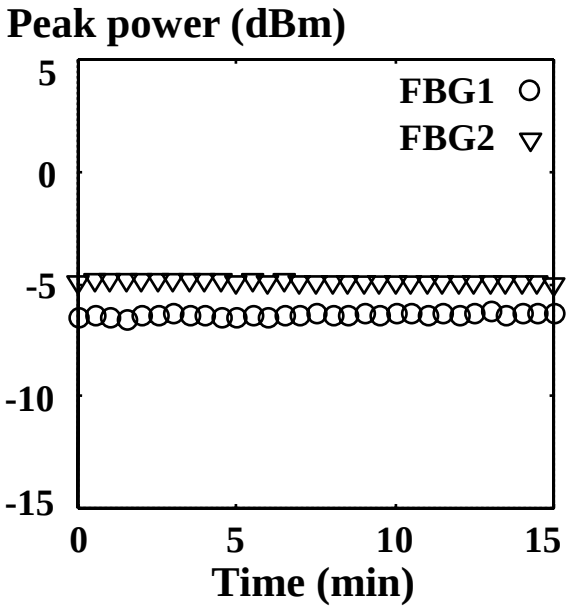

Fig. 4.11 Variation of peak power as a function time for each lasing line.

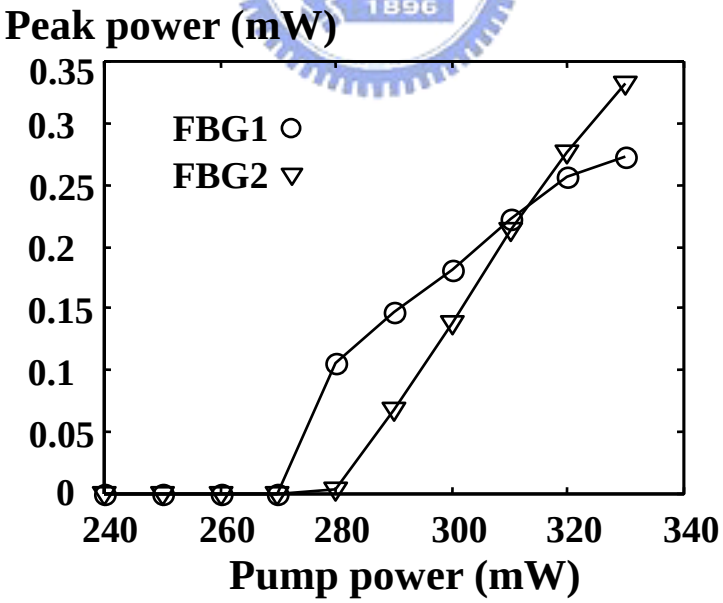

Fig. 4.12 The relationship between the peak power and the Raman pump power.

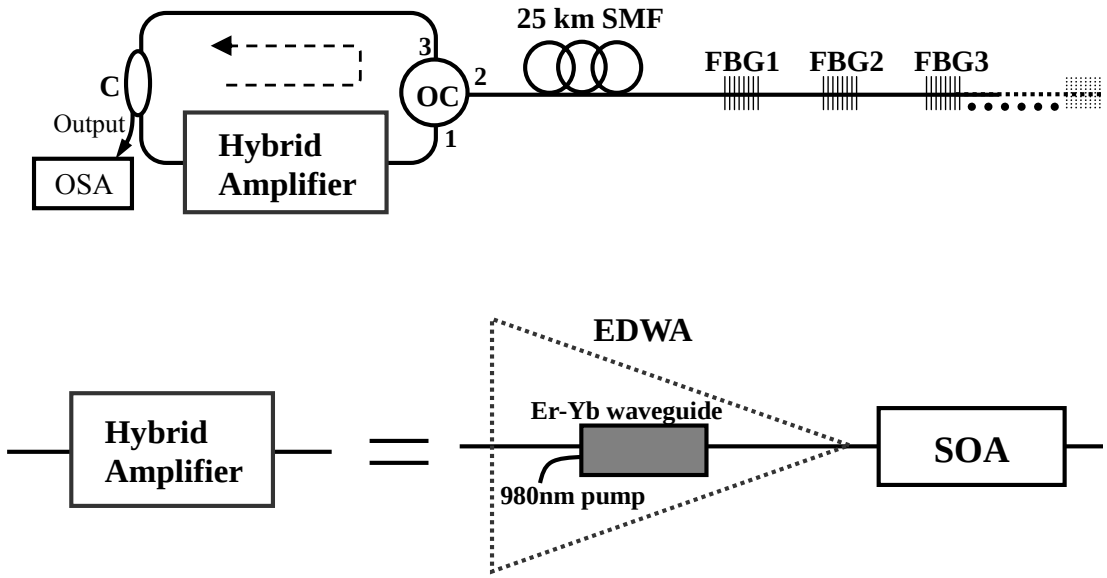

Fig. 4.13 Schematic diagram of the long-distance FBG sensor system. (OSA: optical spectrum analyzer, C: 1x2 coupler with coupling ratio 90:10, OC: optical circulator, SMF: single mode fiber, EDWA: erbium doped waveguide amplifier, SOA: semiconductor optical amplifier).

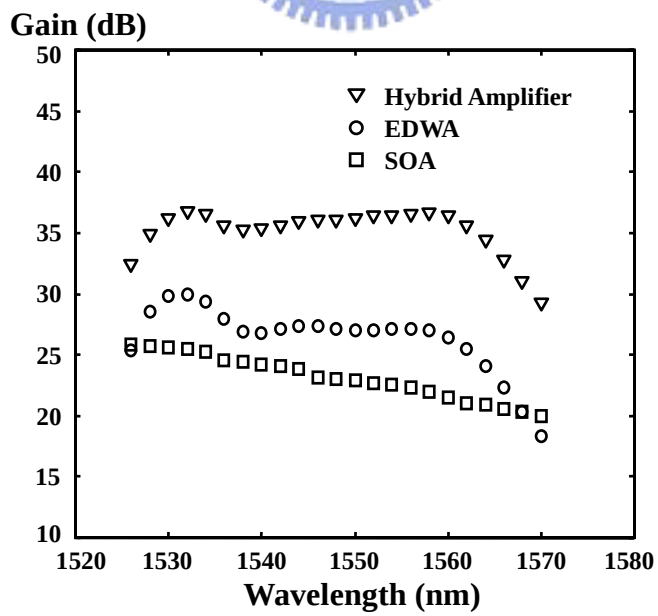

Fig. 4.14 Optical gain spectra of the EDWA, SOA, and hybrid amplifier when the input power is set at -25 dBm.

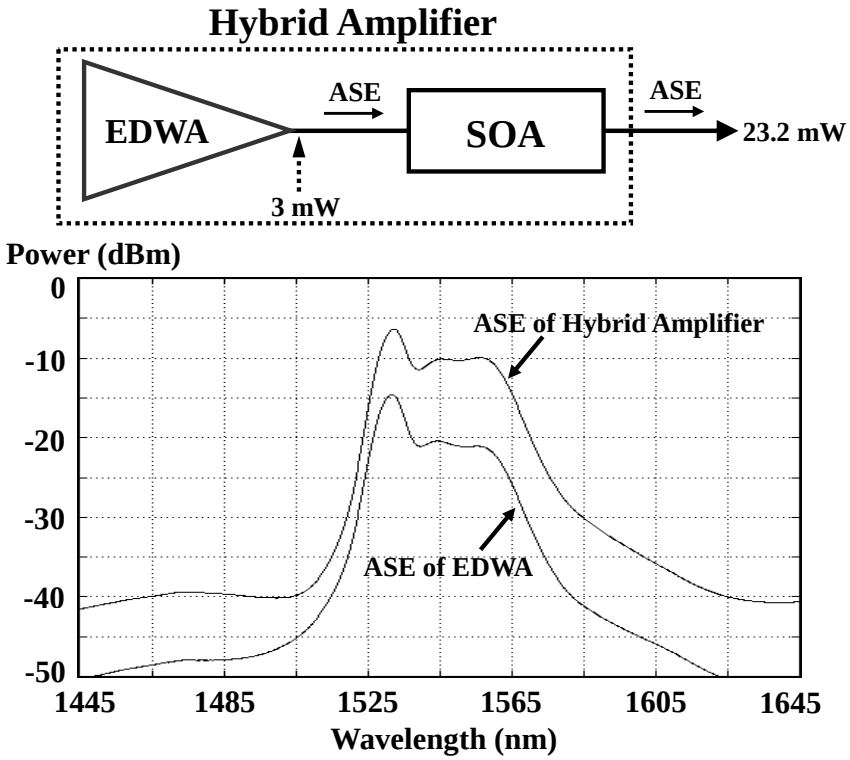

Fig. 4.15 ASE spectra of the EDWA and hybrid amplifier.

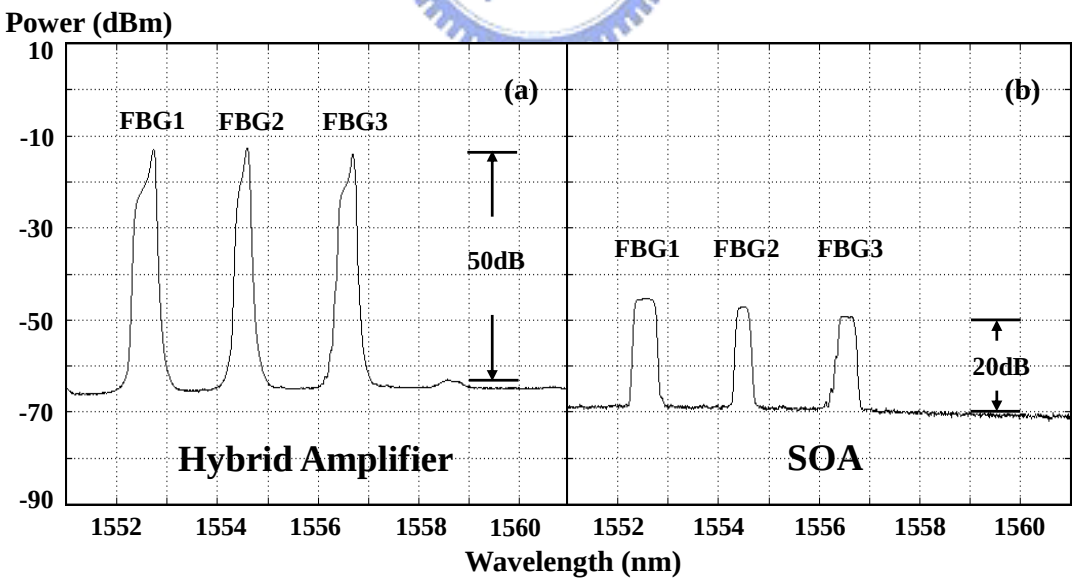

Fig. 4.16 Output spectra of the fiber ring laser with (a) hybrid amplifier and (b) SOA.

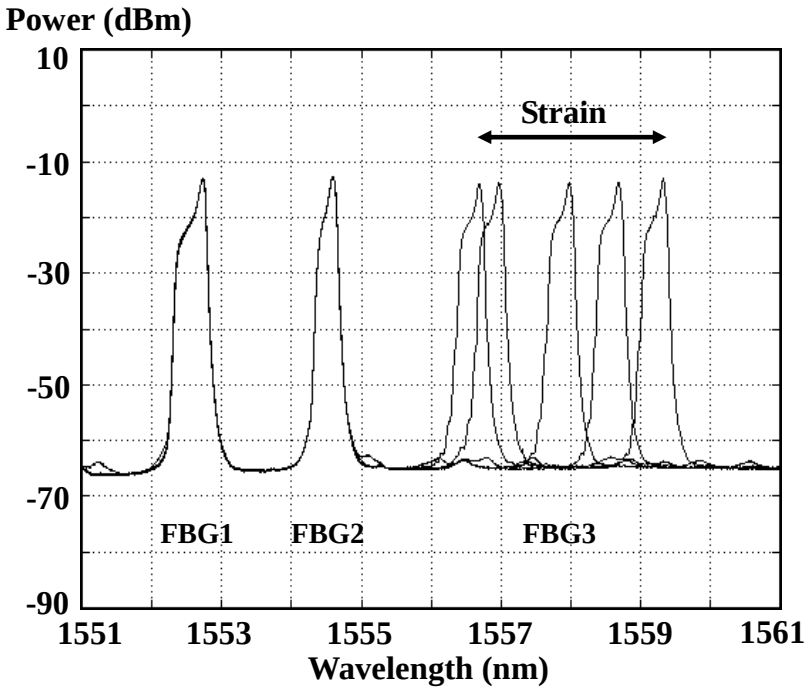

Fig. 4.17 Wavelength shifts of FBG3 when different strains were imposed on it.

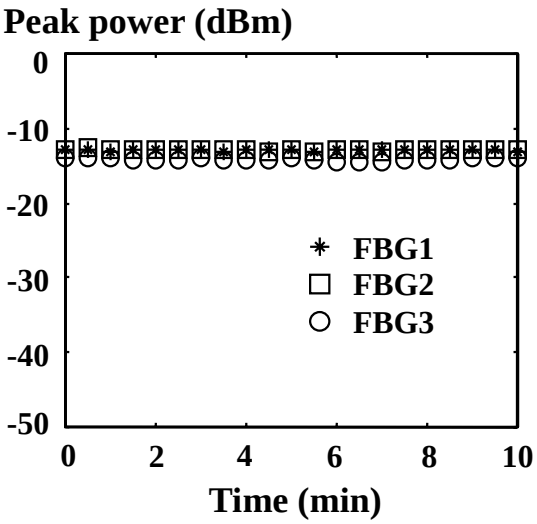

Fig. 4.18 Variation of peak power as a function time for each lasing wavelength.